ELSEVIER

Medical Image Analysis 6 (2002) 361–373

MEDICAL IMAGE ANALYSIS

www.elsevier.com/locate/media

Model-driven brain shift compensation

Oskar Škrinjar[a,*], Arya Nabavi[b], James Duncan[c]

[a]*Department of Electrical Engineering, Yale University, New Haven, CT, USA*
[b]*Surgical Planning Laboratory, Brigham and Women's Hospital, Harvard University, Boston, MA, USA*
[c]*Department of Diagnostic Radiology, Yale University, New Haven, CT, USA*

Received 10 December 1999; received in revised form 17 August 2001; accepted 26 October 2001

Abstract

Surgical navigation systems provide the surgeon with a display of preoperative and intraoperative data in the same coordinate system. However, the systems currently in use in neurosurgery are subject to inaccuracy caused by intraoperative brain deformation (brain shift), since they typically assume that the intracranial structures are rigid. Experiments show brain shift of up to 1 cm, making it the dominant error in the system. We propose a biomechanical-model-based approach for brain shift compensation. Two models are presented: a damped spring–mass model and a model based on continuum mechanics. Both models are guided by limited intraoperative (exposed brain) surface data, with the aim to recover the deformation in the full volume. The two models are compared and their advantages and disadvantages discussed. A partial validation using intraoperative MR image sequences indicates that the approach reduces the error caused by brain shift.
© 2002 Elsevier Science B.V. All rights reserved.

Keywords: Brain shift modeling; Soft tissue deformation; Spring–mass model; Continuum mechanics model

1. Introduction

The use of surgical navigation systems has become a standard way to assist the surgeon in navigating within the intraoperative environment, planning, and guiding the surgery. One of the most important features of these systems is the ability to relate the position of surgical instruments to features in preoperative images. Ideally, they should provide a 3D display of the neuroanatomical structures of interest and include visualization of surgical instruments within the same coordinate system. In order to be reliably used, surgical navigation systems should be as accurate as possible, preferably to within the voxel size of the used images (Grimson et al., 1996). Most of the current systems use preoperatively-acquired 3D data and register it to the patient coordinate system (Grimson et al., 1995, 1996; Peters et al., 1996). However, they assume that the organs being operated on are rigid, and are consequently subject to error due to the soft tissue deformation.

In this paper, we concentrate on the problem of compensation for brain deformation during the surgery (commonly referred to as brain shift), although a similar approach can be applied to other related problems involving soft tissue deformation. Preoperative data are registered to the patient coordinate system at the beginning of the surgery. While this can be done with a precision to within 1 mm at the beginning of the surgery (Grimson et al., 1996), since the brain deforms, the accuracy of the system deteriorates as the surgery proceeds. The median brain shift after the dura had been opened of points on the brain surface was estimated to range from 0.3 to 7.4 mm (Hill et al., 1997). Since the deeper brain structures deform less than the outer ones, the largest error is at the cortical surface. It is clear that a surgical navigation system based on the rigid brain assumption cannot achieve a precision better than a few millimeters in the outer brain structures. The brain deforms even more after interventions (e.g.

*Corresponding author.
E-mail address: oskar.skrinjar@bme.gatech.edu (O. Škrinjar).

1361-8415/02/$ – see front matter © 2002 Elsevier Science B.V. All rights reserved.
PII: S1361-8415(02)00062-2

post-resection). Furthermore, the average brain shift for cases in which hematoma or tumors were removed was reported to be 9.5 and 7.9 mm, respectively (Bucholz et al., 1997). In such cases the error is even larger.

Brain shift contributes to the inaccuracy of surgical navigation systems more than any other source of error. Since the accuracy of surgical navigation systems is the top priority in making them useful, this problem has been addressed by several groups. The initial work was on estimating and reporting brain shift (Bucholz et al., 1997; Dorward et al., 1997; Hata et al., 1999; Hill et al., 1997; Maurer et al., 1998a; Reinges et al., 1997; Roberts et al., 1998), while later efforts were aimed at compensating for the brain shift using a deformable model (Edwards et al., 1997; Miga et al., 1998, 1999, 2000; Škrinjar et al., 1998; Škrinjar and Duncan, 1999; Škrinjar et al., 2001) and intraoperative brain imaging (Gobbi et al., 1999; Hata et al., 1999; Hill et al., 1999; Maurer et al., 1998; Nabavi et al., 2001). We also note related work on: modeling of brain deformation due to tumor growth (Kyriacou and Davatzikos, 1998), biomechanical model based non-rigid registration of brain images (Ferrant et al., 2000; Hagemann, 2001), finite element modeling of the head under impact conditions (Claessens, 1997), and brain tissue constitutive modeling (Miller and Chinzei, 1997).

Brain shift is a complex phenomenon, and here we list factors that, not necessarily in the order of importance, affect brain deformation: gravity, mechanical tissue properties, administered drugs, loss of cerebro-spinal fluid (CSF), interaction of CSF and brain tissues, anatomical constraints, tissue resection and removal, intracranial pressure, geometrical complexity, and patient variability. Given this list, it becomes obvious that it is virtually impossible to reliably model brain deformation without use of intraoperative information. This assumption is the basis of our approach. Similar observations were reported in (Hill et al., 1999). The use of intraoperative information for model guidance was suggested by a few groups (Audette et al., 1999; Edwards et al., 1997; Maurer et al., 1998a; Škrinjar and Duncan, 1999; Škrinjar et al., 2001). Although there are surgical navigation systems that use intraoperative data, e.g. input from intraoperative scanners (Gering et al., 1999; Kansy et al., 1999), they do not update available preoperative images (high resolution preoperative MRI, CT, MRA, fMRI, PET, SPECT and others) when the brain deforms, and therefore the precision with which they display preoperative data is still limited by the error due to brain shift.

Here, we present an approach for dealing with the problem of brain shift that relies on a combination of intraoperative input and a biomechanical deformable brain model. We start by giving an overview of the general steps needed for the approach. Then we introduce a damped spring–mass brain model guided by sparse points delineated on the exposed brain surface, and point out drawbacks of this method. In order to overcome the drawbacks, we move to a continuum mechanics based brain model guided by exposed brain surface data. We compare the two models and discuss their advantages and disadvantages. Finally, we present a partial validation of the continuum mechanics based brain model using intraoperative MR image sequences.

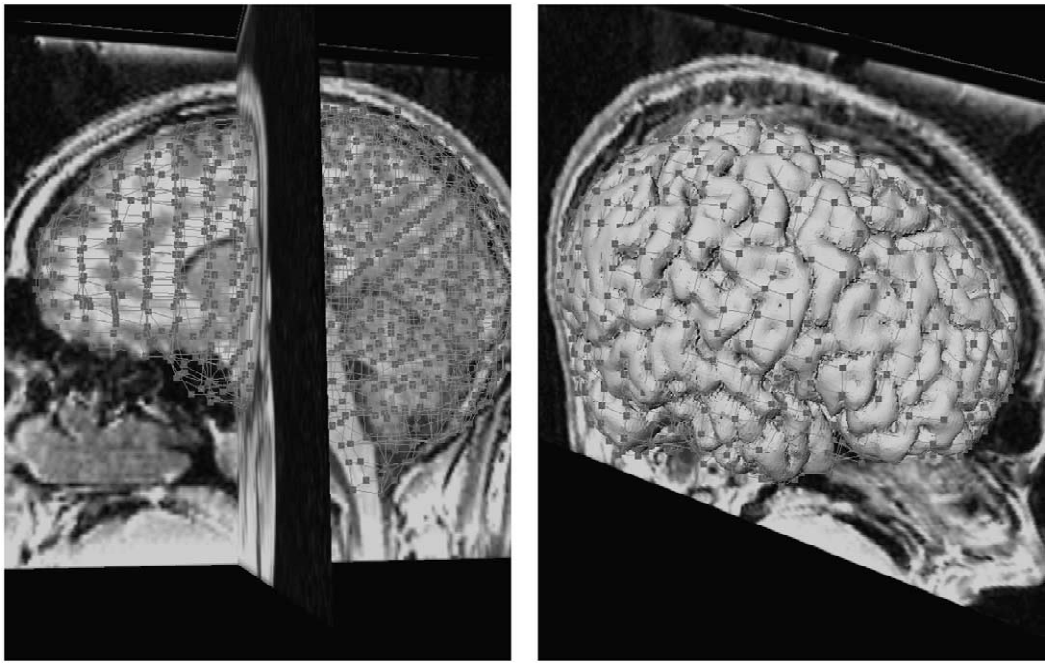

Fig. 1. A typical model mesh. The left figure shows the mesh, while the right one shows the mesh and the outer brain surface. The mesh has over 2000 nodes and 1500 elements (bricks).

2. System overview

Our approach to brain shift compensation is to run an intraoperatively guided 3D brain model during the surgery and use the model output to display preoperative data (deformed according to the current model state). Before the surgery one can acquire anatomical (MRI, CT) and functional (functional MR, SPECT, PET, etc.) images, segment them, generate surfaces of the segmented structures of interest, and then deform all of them intraoperatively based on the current model state. If the model deformation prediction is close to the actual brain deformation, then the displayed images and structures of interest (that are deformed according to the current model state) are closer to the current actual brain state than they would be if one did not use the brain shift compensation, making the surgical navigation system more precise and reliable.

Therefore, we propose a biomechanical-model-based brain shift compensation system composed of the following tasks: preoperative image acquisition, segmentation, mesh generation, registration of the model to the intraoperative environment, model setup and guidance, and visualization of model-updated preoperative data.

2.1. Segmentation, visualization and registration

The first step after the preoperative image acquisition is the segmentation of the brain tissue. For this task we have adopted the automatic brain segmentation algorithm suggested in (Stokking, 1998), enhanced by a few pre- and post-processing steps.

For object surface rendering we have used an improved version of the algorithm presented in (Gibson, 1998). Some of the surfaces produced by this algorithm can be seen in Figs. 1–3.

In order to display and use brain surface data for model guidance, a rigid body transformation between the patient and preoperative image coordinate systems has to be established. For this purpose we used a set of fiducial markers placed on the patient's skin. In the operating room (OR), the marker coordinates were recorded using a mechanical localizer (Operation of Mayfield, 1997). In addition, the markers were manually localized in the preoperative MRI dataset.[1] Then a robust point matching algorithm for resolving the correspondences and finding the optimal rigid body transformation between the two sets of marker locations was applied (there are many point matching algorithms suggested in the literature, see e.g. (Chi et al., 1999)). Once the rigid body transformation is determined, any point recorded by the localizer can be mapped to the preoperative image coordinate system.

2.2. Mesh generation

The next step is to generate the model mesh from the segmented brain tissue. Here we use hexahedral ('brick') elements,[2] having *eight* nodes at the vertex positions. The segmented object (the brain tissue in this case) is the input to our mesh generator, which generates an unstructured

[1] Markers have to be imageable in MR and/or CT scanners.

[2] The term 'brick element' (or just 'brick') is used in FEM analysis, and we use it for the continuum mechanics-based brain model, since we solve it using a FEM. However, we use the same term ('brick element') for the spring–mass model, since the nodes are organized in 'bricks', and the 'brick' mesh structure is used for the trilinear interpolation. We hope that there will be no confusion because the two models are described separately.

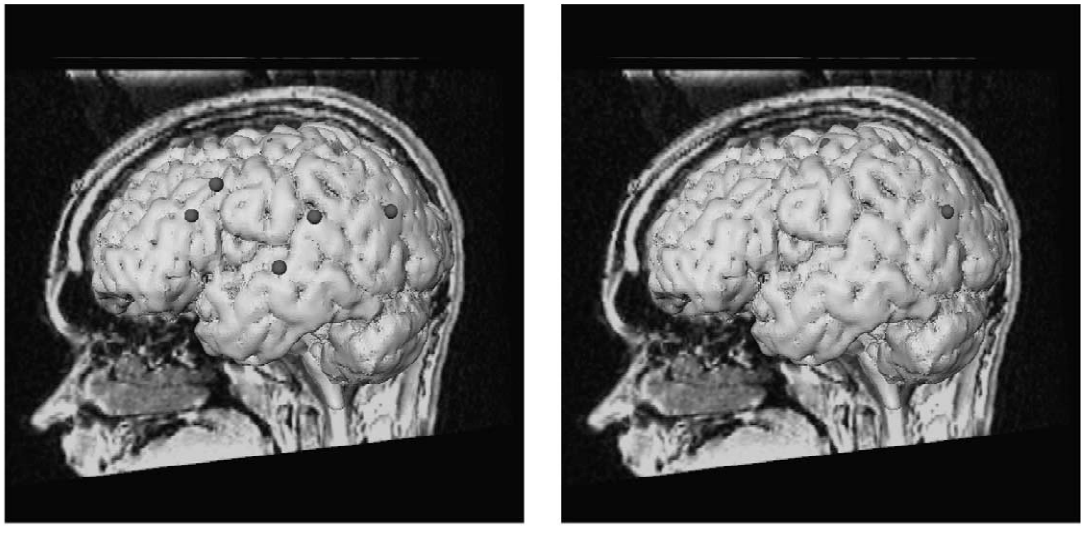

Fig. 2. Intraoperatively recorded points on the exposed brain surface at the beginning of the surgery are shown at left, while their positions about 45 min later relative to the same pre-deformation brain surface are shown at right. Gravity is perpendicular to the sagittal plane. The points moved in the direction of gravity and they are hidden under the pre-deformation brain surface (only one of the points is still visible in the figure at right). Since the brain deformed (in the direction of the gravity vector), the surface points moved relative to the pre-deformation brain surface.

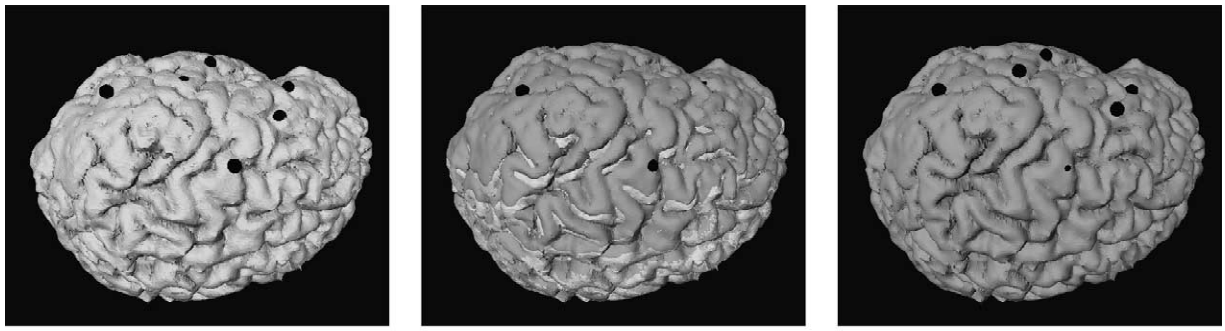

Fig. 3. An example of a guided brain deformation model output. (a) The recorded points at the beginning of the surgery with the initial (pre-deformation) brain surface. Note that the points are on the brain surface. (b) The final (steady state) brain surface points with initial brain surface (darker surface) and final brain surface (lighter surface). One can see that the brain surface points moved inside the initial brain surface. This is due to the effect of gravity that pulled the brain downwards. (c) The final brain surface points and final brain surface after model-guided updating. The points are again on the brain surface. The final brain model surface was computed using the final model state, while the final points are the measurements on the brain surface when the brain settled down.

mesh (Liseikin, 1999). The algorithm first generates a regular 3D matrix of bricks over the full 3D image. Each brick that has at least a half of its volume inside the segmented object is kept, and others are discarded. The kept bricks will compose the final mesh, while their nodes will be finely readjusted. The nodes are divided into two groups. Each node that has all of its neighboring nodes left is called an interior node, and all other nodes are called surface nodes. Each surface node is moved to the closest point on the surface of the segmented object. Note that surface nodes before moving were not far from the surface of the segmented object. Finally, the interior nodes are smoothed using a Laplacian-type smoother[3] (Liseikin, 1999), in order to enhance the regularity of the mesh. A typical output of the mesh generator is shown in Fig. 1. The meshes we use do not capture all of the fine details of the segmentation output, but they still achieve a reasonable performance in terms of accuracy and speed. A much finer mesh, that would capture all brain geometric details (e.g. sulcul structures), would have too many nodes and would slow down the computation, while not achieving a significant improvement in accuracy.

2.3. Intraoperatively-guided biomechanical brain model

In our initial efforts to recover intraoperative brain deformation we used a damped spring mass model (see Section 3.1 for details) for its simplicity, speed, and ability to model slow and small soft tissue deformation. As we further explored the problem of brain shift compensation, we moved to a continuum mechanics-based model (presented in Section 3.2) which is also able to recover small soft tissue deformation, and although computationally more expensive, it overcomes drawbacks associated with the former model. Both models are guided by exposed brain surface data. While for the spring–mass model we used a few brain surface points to guide the model, as we advanced to the continuum mechanics-based model we used a surface reconstruction of the exposed brain surface for model guidance.

2.4. Interpolation

The result of solving model equations (explained in later sections) is a set of node displacements over time. One usually wants to display updated (deformed) preoperative images and surfaces of objects of interest. For this purpose we employ trilinear interpolation to determine the displacement field in between model nodes. This interpolation scheme provides C_0 continuity of the displacement field.

It turns out that this task requires both the forward and inverse trilinear interpolation. The forward trilinear interpolation equations can be written in the following matrix form:

$$[x\ y\ z]^{\mathrm{T}} = A[1\ \alpha\ \beta\ \gamma\ \alpha\beta\ \alpha\gamma\ \beta\gamma\ \alpha\beta\gamma]^{\mathrm{T}}, \quad (1)$$

where x, y and z are coordinates in the global coordinate system, while α, β and γ are the corresponding local coordinates in the coordinate system of the 'brick' element. The 24 elements of the 3×8 matrix A depend directly on the (known) displacements at the eight nodes of

[3]Each interior node is moved to the mean position of its neighboring nodes, while surface nodes are kept fixed. This is iteratively repeated until interior nodes achieve a steady state, i.e. until the displacement of the interior node that moved the most in the current iteration is less than a given value.

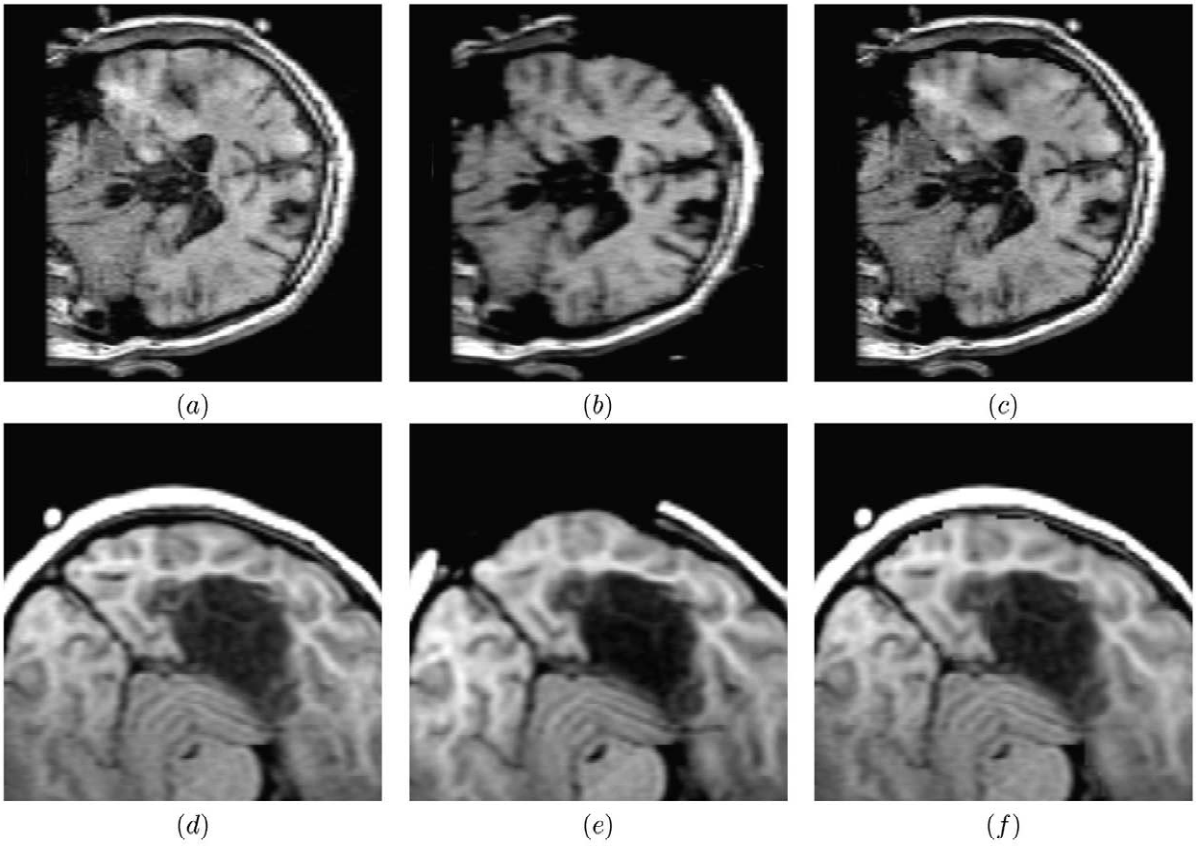

Fig. 4. (a) A preoperative coronal slice of a sinking brain; (b) the corresponding intraoperative slice of the deformed brain; (c) the corresponding model-computed slice of the deformed brain. Axial slices (d), (e) and (f) correspond to the bulging brain case (undeformed, deformed and model-computed, respectively). Note that in both cases the exposed brain surfaced in the computed slice moved similarly as the corresponding surface in the intraoperative slice.

the 'brick' element,[4] and can therefore be considered known.[5] While one just needs to evaluate (1) to do the forward trilinear interpolation, i.e. to obtain the global coordinates for given local coordinates, it is more difficult to do the inverse trilinear interpolation, i.e. to determine the local coordinates for given global coordinates. The inverse problem can be solved explicitly, but the solution expressions are cumbersome (there are three solutions since it is a cubic equation in local coordinates). We have found the explicit solution not practical, and have decided to numerically solve the inverse interpolation. We use an iterative bisection method[6] for this purpose. The method converges rapidly achieving the given precision (0.1 mm) in several iterations.

An example of a deformed surface is given in Fig. 3(b) and (c), while model updated images are shown in Fig. 4(c) and (f).

3. Biomechanical brain model

3.1. A damped spring–mass brain model

In our research we are mainly concerned with (but not limited to) issues surrounding epilepsy surgery. To quantitatively investigate such a case we have recorded a set of six points on the exposed brain surface approximately every 8 min during the surgery starting when the dura was opened. The mean shift in the direction perpendicular to the brain surface was about 3 mm. The initial and final[7] set of points both displayed over the same pre-deformation brain surface generated from a preoperative MR scan are shown in Fig. 2. This result clearly shows the need for a high quality intraoperative 3D acquisition system and/or a method for brain shift compensation. Trade-offs among different approaches to these problems are discussed later in the paper.

[4]The displacements at the nodes of the 'brick' element are determined by solving the model equations.

[5]Their computation is straightforward (the local coordinates take values 0 or 1 at the eight 'brick' nodes).

[6]We do the bisection search in the three local coordinate directions (see Press et al., 1992).

[7]By initial moment we mean the moment when the dura was opened, and the final moment is when the brain settled down and achieved a steady state.

The approach we have taken is to use a biomechanical deformable model that models the brain soft tissue, incorporates the effects of gravity, and can be guided by intraoperative measurements. Since the goal was to perform brain deformation compensation in real-time, i.e. faster or equal to the real brain deformation, we decided to use a damped spring–mass model because of its speed and ability to model small[8] soft tissue deformation.

3.1.1. Model

3.1.1.1. Brain tissue modeling. According to our findings and findings of other groups (Bucholz et al., 1997; Hill et al., 1997) brain shift is a relatively small deformation and a slow process. This fact facilitates our approach to brain tissue modeling. We employ a linear stress–strain relation, which is a good approximation for a small tissue deformation. The model consists of a set of discrete interconnected nodes each representing a small part of the brain tissue. Nodes have masses depending on the size of the volume they represent and on the local tissue density. Each connection is modeled as a parallel connection of a linear spring and dashpot, known as the Kelvin solid model (Pamidi and Advani, 1978). As for the nodes, the connection parameters can depend on their position in the brain. The Kelvin solid model is a model for a viscoelastic material subject to slow and small deformations, which is exactly the case with brain shift. It is also a rather simple approach, which is a desirable property since the model deformation should be computed in real time, i.e. faster or at least at the speed of the brain deformation, since it must be utilized (e.g. the resulting volumetric deformation displayed) during the surgery. The constitutive relation for the Kelvin solid model is

$$\sigma = q_0 \epsilon + q_1 \dot{\epsilon}, \tag{2}$$

where σ is stress and ϵ strain, while q_0 and q_1 are local parameters. The dotted variables represent the time derivatives, e.g. $\dot{\epsilon} = \frac{\mathrm{d}}{\mathrm{d}t}\epsilon$.

Eq. (2) can be rewritten in the following way. If two nodes are at positions $\boldsymbol{r}_1$ and $\boldsymbol{r}_2$, have velocities v_1 and v_2, and are connected in the above fashion, then the force acting on the first node is

$$\begin{aligned} \boldsymbol{f}_{\text{inner}}(\boldsymbol{r}_1, \boldsymbol{r}_2, \boldsymbol{v}_1, \boldsymbol{v}_2) &= \boldsymbol{f}_{\text{elastic}} + \boldsymbol{f}_{\text{viscous}}, \\ \boldsymbol{f}_{\text{elastic}} &= k_s(\|\boldsymbol{r}_2 - \boldsymbol{r}_1\| - r_{12})\,\boldsymbol{n}_{21}, \\ \boldsymbol{f}_{\text{viscous}} &= -k_d[(\boldsymbol{v}_2 - \boldsymbol{v}_1)\cdot \boldsymbol{n}_{21}]\boldsymbol{n}_{21}, \end{aligned} \tag{3}$$

where k_s is the stiffness coefficient, k_d is the damping coefficient, and r_{12} is the rest length of the spring connecting the two nodes. In a general case they can vary from connection to connection depending on the local material properties. $\boldsymbol{n}_{21}$ is the unit vector from $\boldsymbol{r}_1$ to $\boldsymbol{r}_2$. Note that the same force acts on the other node but in the opposite direction.

3.1.1.2. Brain–skull interaction. The brain–skull interaction as modeled in our initial efforts in (Škrinjar et al., 1998), is a highly nonlinear function, and significantly slows down the adaptive step-size numerical integration. The consequence was that the steady-state for this previous 3D model (with about 1000 nodes and 5000 connections) was reached in approximately 4 h, which is much slower than the real brain deformation, and therefore the model cannot be used for display updating during the surgery.

For this reason we now use an alternate approach. Prior to the simulation the skull and brain tissue have to be segmented. Ideally, a preoperative MRI scan would be used for brain tissue segmentation and a preoperative CT scan for skull segmentation (the MR and CT scans would be registered, e.g. by the algorithm suggested in (Studholme et al., 1996)). However, since we didn't have preoperative CT scans available, we did an approximate skull segmentation from preoperative MR images, using a combination of automated and manual processing steps. The brain–skull interaction is not directly a part of the model equations, but rather it is incorporated via numerical integration, through a contact algorithm. As the model evolves over time, when a node enters the skull area, it is returned to its previous position (to its position from the previous step in the numerical integration). This prevents nodes from entering the skull, but permits them to come arbitrarily close to it (more precisely, close up to the precision set in the numerical integration) and move along the skull surface if pulled by forces that are not perpendicular to the skull surface. Effectively, nodes can move freely unless they reach the skull, in which case they can move only in the direction tangential to the skull surface. This behavior is identical to the one achieved by the brain–skull interaction suggested in (Škrinjar et al., 1998), but it is much faster to simulate. As a result, the 3D model now needs about 10 min to reach the steady state, which is faster than the actual brain deformation (which is, according to our surgical colleagues, approximately 45 min).

3.1.1.3. Model equations. Newton's Second Law for each node j in the model gives

$$m^j \boldsymbol{a}^j = m^j \boldsymbol{g} + \sum_{i=1}^{n^j} \boldsymbol{f}^j_{\text{inner}_{s_i^j}}, \tag{4}$$

where m^j is the node's mass, $\boldsymbol{a}^j$ is its acceleration, $\boldsymbol{f}^j_{\text{inner}_{s_i^j}}$ is the interaction between nodes j and s_i^j defined by (3), and $\boldsymbol{g}$ is the gravity acceleration, while $\{s_1^j, s_2^j, \ldots, s_{n^j}^j\}$ is the set of n^j neighboring nodes of the node j. Eq. (4) represents a system of second order nonlinear ordinary differential equations.

One can define state variables to be $\boldsymbol{x}_{2j-1} = \boldsymbol{r}^j$ and $\boldsymbol{x}_{2j} = v^j$ for $j = 1, \ldots, N$, where N is the number of the

[8] Brain shift is small relative to the brain size.

brain model nodes, $\boldsymbol{r}^j$ is the position vector of the jth node, and v^j is its velocity. Obviously, $\dot{\boldsymbol{x}}_{2j-1} = \boldsymbol{x}_{2j}$. The expression for $\dot{\boldsymbol{x}}_{2j}$ can be obtained directly from (4), since $\dot{\boldsymbol{x}}_{2j} = \frac{\mathrm{d}}{\mathrm{d}t}\boldsymbol{x}_{2j} = \boldsymbol{a}^j$. The expression depends only on state variables but not on their time derivatives. It follows that (4) can be rewritten in a compact state–space form, $\dot{\chi} = \boldsymbol{f}(\chi)$, where χ is the vector of the state variables and $\dot{\chi} = \frac{\mathrm{d}}{\mathrm{d}t}\chi$. It is assumed that the brain starts deforming from a rest position, i.e. $v^j(t=0) = \boldsymbol{0}$ for all j. The initial node positions, $\boldsymbol{r}^j(t=0)$, are set by the mesh generator (Section 2.2).

The system in the state–space form is suitable for a numerical integration (Press et al., 1992). In this case the fourth order Runge–Kutta method with adaptive step size was employed. The brain–skull interaction is implicitly included in the numerical integration as explained in the previous section.

3.1.2. Parameter estimation

One of the problems in soft tissue deformation recovery is a reliable model parameter estimation. The approach we have employed here is to use intraoperative measurements to estimate model parameters. Although our model allows for local parameter control, we still assume a homogeneous model for two reasons. First, it is very difficult to estimate the brain tissue parameters locally and, second, there are contradictory reports in the literature regarding white and gray stiffness properties. For our approach, even in the case of a homogeneous model, there are two parameters to be estimated: the stiffness coefficient k_s and the damping coefficient k_d in Eq. (3).

Let $S(t)$ be the brain surface generated by the model at time t, and let $x_i(t)$, $i = 1, \ldots, N$ be the recorded brain surface points (in our case $N = 6$) at time t. Furthermore, let $d(x, S)$ denote the signed distance between the point x and the closed surface S, where $|d(x, S)|$ is the distance between x and S, and $d(x, S)$ is negative if the point is inside the surface, and positive if it is outside. We treat the brain surface as a closed surface. The average signed distance of the recorded points to the brain surface at time t is

$$d(t) = \frac{1}{N}\sum_{1}^{N} d(x_i(t), S(t)), \tag{5}$$

and the total average signed distance (over time) is

$$d = \frac{1}{M}\sum_{1}^{M} d(t_i), \tag{6}$$

where M is the number of times brain surface points were recorded, and t_i, $i = 1, \ldots, M$, are the corresponding times.

We used an off-line parameter estimation, where the whole sequence (over time) of the recorded brain surface points was utilized. Model simulations indicated that the steady state did not depend on the damping coefficient, but only on the stiffness coefficient. This conclusion coincides with the exact mathematical analysis of simple one-object systems (e.g. a mass connected to a spring that is fixed at the other end, with a friction between the mass and the support). The damping coefficient determines how fast the steady state will be reached, while the stiffness coefficient determines the final shape of the brain.

For this reason we use the steady state[9] to estimate the stiffness coefficient. Since reports by other researchers as well as experiments done by our group suggest that the brain shifts mainly in the direction of gravity, we use the following approach to estimate the model parameters. We pick a relatively small value k_1 for the stiffness coefficient, such that $d(t_M)$ (defined by Eq. (5)) is positive.[10] Similarly, we pick a relatively large value k_2 for the stiffness coefficient, such that the corresponding $d(t_M)$ is negative. The next step is to use $k_{\mathrm{new}} = (k_1 + k_2)/2$ as a stiffness coefficient, run the model again, and get a new value for $d(t_M)$. If $d(t_M) > 0$, we set $k_1 = k_{\mathrm{new}}$. Otherwise, we set $k_2 = k_{\mathrm{new}}$. Then we repeat the steps, i.e. continue with the bisection search, until $d(t_M)$ is close enough to zero. The last k_{new} is used as the 'optimal' stiffness coefficient. For all the steps we use an arbitrary value for the damping coefficient since it does not affect the steady state.

Once the stiffness coefficient is estimated, the damping coefficient is determined in a similar fashion (using the bisection search), but this time by using d (defined by Eq. (6)) rather than $d(t_M)$, i.e. by reducing the average signed distance over time.

The idea was to estimate the model parameters on a number of patients and then use their average values for future patients for brain deformation compensation. We intraoperatively recorded exposed brain surface points for four patients, but due to technical difficulties we were able to use the data only of two of them. From the two patients we determined the average model parameter values. These parameter values were used for all the experiments discussed in the paper.

While one could record brain surface points for more patients and get a possibly better estimate for the model parameters, there are a few problems related to this approach. The main problem is that the model parameters are mesh dependent, i.e. if one wanted to use a denser (or sparser) mesh, he would need to readjust the model parameters to achieve the same model behavior. However, it is not clear how to mathematically readjust the model parameters for a denser mesh, except for a 1D model. For the same reason one cannot use a non-uniform mesh (mesh with different node densities in different regions). Since

[9] The time of the steady state is t_M, and it denotes the time when the last set of points was recorded (after the brain settled down, i.e. achieved a steady state).

[10] For a small stiffness coefficient the model is 'soft', and it will settle down significantly, i.e. more than the actual brain, causing all the recorded points at time t_M to be outside the brain model surface. For this reason each point will have a positive signed distance to the brain model surface.

Table 1
Average brain surface movement and model error

	Time [min:s]							
	0:00	7:40	14:40	19:40	24:40	34:52	49:00	Max
Surface movement [mm]	0.34	1.38	2.21	2.30	2.74	3.24	3.29	3.29
Model error [mm]	0.34	0.45	0.30	0.13	0.20	0.32	0.04	0.45

the model parameters are mesh dependent they cannot be found in the literature. Furthermore, if we want to use the average values for the model parameters estimated from a number of patients, we would need to use model meshes of the same density for all the patients. Mesh dependence of the model parameters is one of the reasons why we have decided to move to continuum mechanics based modeling, rather than further investigating damped spring–mass models. Model parameters in continuum mechanics based models are mesh independent, which avoids all the mentioned problems.

Table 1 shows the average distance between the rigid (initial) gray/CSF brain surface and recorded brain surface points over time (i.e. during the operation) in the row 'surface movement'. In addition, the row 'model error' contains the average error between the model predicted position of the gray/CSF brain surface and the positions of the recorded brain surface points over time. This table contains data for a single patient undergoing epileptic (implant) surgery. The surgeon touched six points (recorded their positions with the mechanical localizer) every 8 min (on average). One can see that the distance between the initial gray/CSF brain surface and the recorded brain surface points increases over time and ultimately reaches 3.29 mm. The model with optimal parameter settings (determined in the off-line way on two patients) has maximal error of 0.45 mm over time. While the error between the model prediction and the actual surface points is relatively small, one should keep in mind that the model parameters were estimated on just two patients, and that the results shown in Table 1 present almost the best fit of the model to the measured points on the brain surface of one of the two patients.

3.1.3. Intraoperative model guidance

In addition to estimating model parameters in an optimal sense, one can guide the model by intraoperative data. The idea is to readjust the model whenever intraoperative measurements are available, and in between measurements to let the model deform on its own. The model tries to predict the node positions at the moment of the new measurements, new measurements are then used to readjust the model, and so on. The denser the intraoperative data are both in space and time the smaller the error between the model and the actual brain position.

In order to guide the model when (at time t) a new set of brain surface points is recorded, we do the following. For each point $x_i(t)$, we compute the displacement vector from the closest point p_i on the brain model surface $S(t)$ to the point $x_i(t)$, and then artificially apply the displacement vector to the surface node closest to the point p_i. The imposed displacement constraints will propagate to other nodes through spring connections as the numerical integration proceeds. By doing this, one brings the model surface closer to the intraoperatively acquired brain surface points. An example of a guided brain deformation model output is shown in Fig. 3.

The problem with this model guidance strategy is that it is completely ad hoc, and it is not clear what the best way is to guide spring–mass models by (intraoperative) surface data. This is the second major reason (the first one was the fact that model parameters are mesh dependent) for moving to continuum mechanics-based models. In the case of latter models, the surface measurements can be used as displacement boundary conditions for the model partial differential equations. This is both mathematically and physically a correct way of guiding the model by surface data.

To validate the approach one would need to obtain for multiple subjects dense time sequences of 3D brain images using intraoperative sensing, and then compare the model predictions to the actual deformations in the full brain volume. This can be done by using intraoperative MRI data, or maybe data from an intraoperative CT or ultrasound scanner.

However, since the only available intraoperative data for these experiments are exposed brain surface points recorded over time, we randomly selected two of the points to guide the model and compared the model predictions against other four points. The results are given in Table 2.

Table 2
Average brain surface movement and model error

	Time [min:s]							
	0:00	7:40	14:40	19:40	24:40	34:52	49:00	Max
Surface movement [mm]	0.34	1.38	2.21	2.30	2.74	3.24	3.29	3.29
Guided model error [mm]	0.34	0.12	0.38	0.44	0.35	0.49	0.14	0.49

Although the error for the guided model is reduced with respect to the case with no brain compensation, this test was done only on one patient, and with very sparse (both in time and space) intraoperative data. An extensive validation using intraoperative volumetric imaging is necessary to determine the reliability of this approach.

The model presented in this section is able to run in real time.[11] The used model meshes had over 2000 nodes, 11 500 connections, and 1500 elements (bricks), and it took less than 10 min on an Octane SGI workstation (R10000 250 MHz processor) to reach a steady state. This is a significant improvement over our previous model (Škrinjar et al., 1998).

3.2. A continuum mechanics based brain model

In spite of the advantages of spring–mass models, we have decided to move to continuum mechanics based models for two aforementioned very important reasons: their parameters are independent of the model mesh and their ability to be guided in a mathematically and physically correct way (though displacement boundary conditions for the underlying model PDEs). Another advantage of the continuum mechanics-based models is their ability to control the tissue incompressibility (through Poisson's ratio), while it is not clear how to do it in the case of spring–mass models.

Our experience with the damped spring–mass brain model suggests that one can neglect dynamic components (components involving velocity and acceleration) in the model, since the brain shift is a relatively slow process. This simplifies the model, and eliminates the need for dynamic model parameters (e.g. damping coefficient). Whenever new intraoperative measurements become available one can solve the model equations constraining (guiding) them by the measurements, and then update preoperative images and surfaces.

We base our approach on the following three assumptions:

- *Relatively simple model*. Due to the complexity of the brain shift phenomenon, not only that it is difficult to model some of the causing factors, but also it is not clear how to set the model parameters (any increase in the model complexity inevitably involves more parameters). Therefore, we base our approach on a simple model, that incorporates the main tissue characteristics (elasticity and almost incompressibility). The complexity of the deformation is made up by intraoperative guidance of the model.
- *Static model*. Since intraoperative brain deformation is a relatively slow process with negligible dynamic components, we use a static model.
- *Intraoperative input*. The model has to by guided by intraoperative input.

There are different types of intraoperative data available for model guidance: points (e.g. using a localizer and recording brain surface points over time, as presented in Section 3.1), surface data: obtained by a range system (Audette et al., 1999) or by a stereo camera system (Škrinjar et al., 2000), and volumetric data obtained by intraoperative image acquisition systems (intraoperative MRI, CT, and ultrasound). One can also take only single 2D images using intraoperative scanners, obtaining 2D (planar) data (Kansy et al., 1999).

For this model we use a pair of stereo cameras overlooking the exposed brain surface to acquire intraoperative information about the deforming brain. The idea is to reconstruct and track the exposed brain surface as it deforms during the surgery. If this can be done reliably, one can use the reconstructed brain surface as displacement boundary conditions for the model PDEs. Each time the surgeon moves her or his hands and surgical tools out of the way of the cameras, snapshots from the two cameras are taken, exposed brain surface is reconstructed, the surface is used to guide the model, and once the model is deformed, it can be used to update (properly warp) all preoperative images available. The advantage of this intraoperative data acquisition over the manual point delineation (Section 3.1) is that it is automated, less disturbing for the surgeon, and it provides more data.

In this section we will not present a complete stereo-guided brain deformation compensation system, but rather we will investigate how well a continuum mechanics-based brain model can predict in-volume deformation using only partial (exposed brain) surface data for model guidance.

3.2.1. Model

Brain shift is a small deformation relative to the brain size, and it is a good approximation to use a linear stress strain relation and infinitesimal strain. Although brain tissues are not isotropic, especially white matter due to its fibrous structure, since the fiber directions are not currently available to us, we assume that brain tissues are isotropic materials. Due to the toughness of falx and tentorium, the movement of the two structures is negligible in most cases. For this reason, we fix the corresponding parts of the model, i.e. we consider only the brain hemisphere on the side of the craniotomy, and assume that the other brain parts do not deform. Furthermore, since brain deformation

[11] By real time we mean the following. The brain deforms with certain speed (it takes about 45 min to assume a steady state). On the other hand it takes a certain time to simulate the brain deformation on a computer, i.e. to deform the model. However, at say 8 min after opening the dura (8 min of the actual, surgical time) the corresponding model state (the state that corresponds to the 8th minute of the actual time) has already been computed and stored in the memory, and can be used for displaying (deformed) images and surfaces. Thus, the simulation of the brain deformation is computed faster than the actual brain deformation, i.e. in real time. If this is not the case, i.e. if the simulation of brain takes more time than the actual brain deformation, then the model could not be used during the surgery (in real time) for displaying deformed images and surfaces.

is a relatively slow process with negligible dynamic components, we use a static model.

The linear stress–strain relation for isotropic materials is given by

$$\boldsymbol{\sigma} = \boldsymbol{C}\boldsymbol{\epsilon}, \tag{7}$$

where $\boldsymbol{\sigma} = [\sigma_x\ \sigma_y\ \sigma_z\ \tau_{xy}\ \tau_{yz}\ \tau_{zx}]^{\mathrm{T}}$ is the stress vector, $\boldsymbol{\epsilon} = [\epsilon_x\ \epsilon_y\ \epsilon_z\ \gamma_{xy}\ \gamma_{yz}\ \gamma_{zx}]^{\mathrm{T}}$ is the strain vector, and $\boldsymbol{C} = \frac{E}{(1+\nu)(1-2\nu)}\boldsymbol{G}$ is the material stiffness matrix, with

$$\boldsymbol{G} = \begin{bmatrix} 1-\nu & \nu & \nu & 0 & 0 & 0 \\ \nu & 1-\nu & \nu & 0 & 0 & 0 \\ \nu & \nu & 1-\nu & 0 & 0 & 0 \\ 0 & 0 & 0 & \frac{1-2\nu}{2} & 0 & 0 \\ 0 & 0 & 0 & 0 & \frac{1-2\nu}{2} & 0 \\ 0 & 0 & 0 & 0 & 0 & \frac{1-2\nu}{2} \end{bmatrix}.$$

The material stiffness matrix depends on two parameters, Young's modulus (E) and Poisson's ratio (ν) (Valliappan, 1981). The displacement vector $\boldsymbol{u} = (u_x\ u_y\ u_z)$ is related to the strain vector through the following equation:

$$\boldsymbol{\epsilon} = \begin{bmatrix} \frac{\partial}{\partial x} & 0 & 0 \\ 0 & \frac{\partial}{\partial y} & 0 \\ 0 & 0 & \frac{\partial}{\partial z} \\ \frac{\partial}{\partial y} & \frac{\partial}{\partial x} & 0 \\ 0 & \frac{\partial}{\partial z} & \frac{\partial}{\partial y} \\ \frac{\partial}{\partial z} & 0 & \frac{\partial}{\partial x} \end{bmatrix} \boldsymbol{u}. \tag{8}$$

Since a static model is assumed, the equations relating stress components and body force are equilibrium equations,

$$\begin{aligned} &\frac{\partial\sigma_x}{\partial x} + \frac{\partial\tau_{yx}}{\partial y} + \frac{\partial\tau_{zx}}{\partial z} + F_x = 0, && \tau_{yx} = \tau_{xy}, \\ &\frac{\partial\tau_{xy}}{\partial x} + \frac{\partial\sigma_y}{\partial y} + \frac{\partial\tau_{zy}}{\partial z} + F_y = 0, && \tau_{zx} = \tau_{xz}, \\ &\frac{\partial\tau_{xz}}{\partial x} + \frac{\partial\tau_{yz}}{\partial y} + \frac{\partial\sigma_z}{\partial z} + F_z = 0, && \tau_{zy} = \tau_{yz}, \end{aligned} \tag{9}$$

where $\boldsymbol{F} = (F_x, F_y, F_z)$ is a body force (gravity in this case).

We are interested in obtaining the displacement field for the brain (to be able to update the preoperative images correspondingly), and therefore the goal is to obtain equations in displacements only. By using the systems of Eqs. (7), (8) and (9), and by eliminating stress and strain components, one can obtain

$$\begin{aligned} &\nabla^2 u_x + \frac{1}{1-2\nu}\frac{\partial}{\partial x}\left(\frac{\partial u_x}{\partial x} + \frac{\partial u_y}{\partial y} + \frac{\partial u_z}{\partial z}\right) + \frac{F_x}{\mu} = 0, \\ &\nabla^2 u_y + \frac{1}{1-2\nu}\frac{\partial}{\partial y}\left(\frac{\partial u_x}{\partial x} + \frac{\partial u_y}{\partial y} + \frac{\partial u_z}{\partial z}\right) + \frac{F_y}{\mu} = 0, \\ &\nabla^2 u_z + \frac{1}{1-2\nu}\frac{\partial}{\partial z}\left(\frac{\partial u_x}{\partial x} + \frac{\partial u_y}{\partial y} + \frac{\partial u_z}{\partial z}\right) + \frac{F_z}{\mu} = 0, \end{aligned} \tag{10}$$

where $\mu = E/2(1+\nu)$. These three equations are elliptic PDEs in displacements only and are known as Navier equations (Valliappan, 1981).

We need to solve Eq. (10) with given displacement boundary conditions. Since they are linear PDEs, and since differentiation is a linear operator, one can separately find the solution $\boldsymbol{u}' = (u_x', u_y', u_z')$ for the equations with zero boundary conditions, and the solution $\boldsymbol{u}' = (u_x'', u_y'', u_z'')$ for the equations with zero body force, and the total solution will be $\boldsymbol{u} = \boldsymbol{u}' + \boldsymbol{u}''$. However, gravity acts all the time, both before and during the brain deformation, and therefore $\boldsymbol{u}'$ will be the same in both cases. Since we are interested in the displacement field between the deformed and undeformed state, we do not need to compute $\boldsymbol{u}'$. Thus, we need to solve only for $\boldsymbol{u}''$, i.e. solve Eq. (10) with the given boundary conditions and zero body force. One should notice that gravity affects $\boldsymbol{u}''$ through boundary conditions (since the brain deforms partly because of gravity, and a part of the brain surface will be used as boundary conditions). Another interesting observation is that Young's modulus does not affect the displacement field ($\boldsymbol{u}''$), since the body force is zero in this case, and therefore the last terms in Eq. (10) containing E (hidden in μ) disappear. Thus, the only model parameter to be set is Poisson's ratio. We have tested a range of values for ν, and the one that yielded the smallest error (a partial validation is presented in Section 3.2.2) was $\nu = 0.4$, which is a value used by other groups as well (Ferrant et al., 2000). We assume that the model is homogeneous since there is no reliable way known to us for setting the model parameter for different brain structures.

3.2.2. Partial validation

In order to test the method, we used intraoperative MR image sequences. We manually segmented the pre-deformation brain regions of interest (cerebral hemisphere at the side of the craniotomy, falx, and tentorium). Then we rigidly registered the preoperative (undeformed) and intraoperative (deformed) brain images using a normalized mutual information based registration algorithm (Studholme et al., 1998). The purpose of this step was to align the undeformed and deformed brain images, i.e. to remove the rotation and translation from the transformation between the two images. We employed a finite element method (Zienkiewicz, 1977) to determine the deformation governed by Eq. (10). A mesh composed of hexahedral ('brick') elements (with 5 mm approximate side lengths) was generated using the segmented data and the in-house

Table 3
Case I (sinking brain) and case II (bulging brain): true landmark displacements ($\boldsymbol{t}$), computed landmark displacements ($\boldsymbol{c}$), and error between true and computed landmark locations ($\boldsymbol{e} = \boldsymbol{c} - \boldsymbol{t}$), for 14 landmarks (all values are in mm)

		Landmarks													
Case		1	2	3	4	5	6	7	8	9	10	11	12	13	14
I	$\|\boldsymbol{t}\|$	0.7	0.9	0.6	0.1	2.3	2.9	2.1	1.0	1.9	2.7	0.8	0.8	2.1	3.8
	$\|\boldsymbol{c}\|$	0.3	0.5	0.7	0.2	1.7	2.4	1.4	0.7	1.3	1.8	0.4	0.5	1.9	3.0
	$\|\boldsymbol{e}\|$	0.8	1.4	0.4	0.2	0.7	1.3	1.4	0.4	1.2	1.3	0.4	0.8	1.0	1.2
II	$\|\boldsymbol{t}\|$	2.7	1.8	0.6	3.6	2.6	0.8	1.3	1.1	1.4	0.7	0.7	0.4	2.4	0.5
	$\|\boldsymbol{c}\|$	2.0	1.6	1.1	2.4	2.6	0.5	0.8	1.2	1.5	0.8	0.5	0.2	2.0	0.3
	$\|\boldsymbol{e}\|$	0.8	1.0	0.6	1.3	0.8	0.4	0.9	0.8	0.9	0.5	0.7	0.5	1.2	0.7

mesh generator explained in Section 2.2. The generated meshes (of the cerebral hemisphere at the side of the craniotomy) had about 6500 nodes and about 5000 'brick' elements. Here we used the anatomical constraints that the falx and tentorium are practically fixed, and we fixed the corresponding model nodes. For this reason it is enough to consider only the half of the brain at the side of the craniotomy, since the other part does not deform. We are aware that, although this assumption holds in most cases, there are exceptions where falx moved during the surgery. In order to simulate exposed brain surface tracking,[12] we manually segmented the deformed brain from the intraoperative scan and generated its surface. Since the brain surface didn't move significantly, we computed the displacement at each point $\boldsymbol{r}_1$ of the undeformed brain surface S_1 (only at the part of the brain surface that was visible through the craniotomy, i.e. at the exposed brain surface), as $\Delta r = \boldsymbol{r}_2 - \boldsymbol{r}_1$, where $\boldsymbol{r}_2$ is the point on the deformed brain surface S_2 closest to the point $\boldsymbol{r}_1$, i.e. obtained as $\arg_{\boldsymbol{r}_2 \in S_2} \min \|\boldsymbol{r}_2 - \boldsymbol{r}_1\|$. Finally, the computed displacements at the exposed brain surface were used as boundary conditions for the model PDEs.

In this section we present a partial validation of the method using intraoperative MRI for two cases:[13] a sinking brain and a bulging brain. For both cases we generated the model and displacement boundary conditions as explained above. We used ABAQUS to compute the model deformation. For a model of about 6500 nodes and about 5000 'brick' elements, it took about 80 s to solve the equations on an SGI Octane R12K machine. This time is almost practically applicable, since it would mean that 1.5 min after obtaining exposed brain surface data, one would get updated MR images and other preoperative data. In order to validate the computed deformation we manually selected a set of anatomical landmarks[14] in the preoperative scan of the (undeformed) brain at various locations throughout the volume of the cerebral hemisphere at the side of craniotomy. Then we manually found the corresponding landmarks in the intraoperative scan of the (deformed) brain. Finally, using the displacement field computed by the model, we determined the positions of the 'model predicted landmarks' in the deformed brain corresponding to the landmarks in the undeformed brain, and compared them to the corresponding manually set landmarks in the deformed brain.

One can see from Table 3 that the maximal true landmark displacement was 3.8 mm (3.6 mm) while the maximal error was 1.4 mm (1.3 mm) for the case of the sinking (bulging) brain. Fig. 4 shows an MR image slice of a preoperative brain, the corresponding intraoperative image slice of the deformed brain, and the corresponding model-updated image slice of the deformed brain. The maximal deformation was at the exposed brain surface (about 7 mm for both cases). However, we did not use landmarks close to the exposed brain surface since the exposed brain surface displacement was used as a boundary condition, and the error at such landmarks would be unrealistically small. Rather, we selected landmarks throughout the volume of the cerebral hemisphere at the side of craniotomy away from the exposed brain surface. This is why the maximal landmark displacement was under 4 mm.

4. Discussion

We presented a brain shift compensation method based on a biomechanical model guided by limited intraoperative data. We started by a simple and relatively fast damped spring–mass brain model. The problems associated with the model parameters and guidance are overcome by an approach that relies on a continuum mechanics-based brain model.

Clearly, this system uses only intraoperative surface information and it cannot perform well after tissue resections. In addition to using this system before resections, one can use it in the case of subdural electrode implantation (often performed as a first stage of epilepsy surgery)

[12] In a complete system brain surface tracking would be done by using a pair of stereo cameras.

[13] In both cases we used intraoperative MR images after the dura was opened and brain deformed, but before any major resection occurred.

[14] For landmarks, we used points at anatomical structures that can relatively easily be identified in both preoperative and intraoperative images.

where no tissue is removed, but the brain still deforms due to gravity, loss of CSF and other mentioned factors.

The approach using continuum mechanics-based brain shift compensation indicates that exposed brain surface information might be enough to recover pre-resection brain deformation with an error comparable to the scan resolution. The used intraoperative MR scans had 2.5 mm slice thickness, with in-plane 0.9375 by 0.9375 mm pixels, while the maximal error of the predicted brain deformation in the presented cases was 1.4 mm.

In addition, this work compares the spring mass and the continuum mechanics-based models for brain shift compensation. The main advantages of the spring mass model are its simplicity and computational efficiency. However, it suffers from mesh dependence on model parameters and from the lack of a good model guidance strategy. Both of the problems are overcome by the continuum mechanics-based model, which disadvantage is that it is computationally more expensive. Another advantage of the latter model is that it can handle not only sinking brain cases, but also bulging ones. Furthermore, it allows for incompressibility control through Poisson's ratio,[15] while it is not clear how to achieve it in the case of the spring–mass model.

As noted above, an alternative to using biomechanical model-based brain shift compensation is to use an intraoperative MRI and/or CT system. Their main advantage is that they provide the actual state of the brain at the time of imaging, i.e. during the surgery, while their disadvantage is that they are very expensive, and therefore not affordable to all hospitals. They also restrict surgical access to the patient, prevent standard metal surgical tools from being used, their spatial resolution is typically not as high as that of preoperative MRI, and one must interrupt the surgery for a few minutes for each image acquisition. Even with the advantages of intraoperative MR scanners, one can see only the current (intraoperative) anatomical state of the brain, but the functional and segmented data is still available only in the preoperative state. Therefore, the use of a deformable model would be helpful even if an intraoperative scanner is available since the model can be guided by the rich intraoperative data from the scanner, and it can correspondingly deform any preoperative data. The main advantages of the use of a deformable model over the use of intraoperative scanners is its much lower cost and its ability to deform any data type, while the main disadvantage is its lower precision and reliability since it is practically impossible to accurately model all the complex phenomena that influence the brain deformation during the surgery.

Our current and future work is aimed at further validation of the approach using additional intraoperative MR image sequences, at reducing the problem of specularities on the wet brain surface (this is a problem in the stereo reconstruction of the brain surface), and at post-resection deformation compensation, for which we believe that intraoperative imaging (MR, CT or ultrasound) is necessary.

[15] Poisson's ratio controls model incompressibility. This parameter is dimensionless, it can relatively reliably be estimated, and its values are available in the literature.

Acknowledgements

We would like to acknowledge the support from Dr. Dennis Spencer and Kevin McCarthy from Department of Neurosurgery, Yale School of Medicine. We are also thankful to Dr. Ron Kikinis, Dr. Ferenc A. Jolesz and Dr. Peter Black from Brigham and Women's Hospital and Harvard Medical School, for collaboration and for providing us with intraoperative MR images.

References

Audette, M.A., Siddiqi, K., Peters, T.M., 1999. Level-set surface segmentation and fast cortical range image tracking for computing intrasurgical deformations. In: Proceedings of MICCAI'99, September, pp. 788–797.

Bucholz, R., Yeh, D., Trobaugh, J. et al., 1997. The correction of stereotactic inaccuracy caused by brain shift using an intraoperative ultrasound device. In: Proceedings of CVRMed-MRCAS'97, Grenoble, France. March, pp. 459–466.

Chui, H., Rambo, J., Schultz, R., Rangarajan, A., 1999. Registration of cortical anatomical structures via robust 3D point matching. In: Proceedings of IPMI'99, June/July, pp. 168–181.

Claessens, M.H.A., 1997. Finite Element Modeling of the Human Head Under Impact Conditions, PhD thesis, Eindhoven University of Technology.

Dorward, N.L., Alberti, O., Velani, B. et al., 1997. Early clinical experience with the Easy-Guide neuronavigation system and measurement of intraoperative brain distortion. In: Hellwing, D., Bauer, B.L. (Eds.), Minimally Invasive Techniques for Neurosurgery, pp. 193–196.

Edwards, P.J., Hill, D.L.G., Little, J.A., Hawkes, D.J., 1997. Deformation for image guided interventions using a three component tissue model. In: Proceedings of the 15th International Conference, IPMI'97, June, pp. 218–231.

Ferrant, M., Warfield, S.K., Nabavi, A. et al., 2000. Registration of 3D intraoperative Mr images of the brain using a finite element biomechanical model. In: Proceedings of MICCAI'2000, October, pp. 19–28.

Gering, D.T., Nabavi, A., Kikinis, R. et al., 1999. An integrated visualization system for surgical planning and guidance using image fusion and interventional imaging. In: Proceedings of MICCAI'99, September, pp. 809–819.

Gibson, S., 1998. Constrained elastic surface nets: generating smooth surface from binary segmented data. In: Proceedings of MICCAI'98, October, pp. 888–898.

Gobbi, D.G., Comeau, R.M., Peters, T.M., 1999. Ultrasound probe tracking for real-time ultrasound/MRI overlay and visualization of brain shift. In: Proceedings of MICCAI'99, September, pp. 920–927.

Grimson, W.E.L., Ettinger, G.J., White, S.J. et al., 1995. Evaluating and validating an automated registration system for enhanced reality visualization in surgery. In: Proceedings of CVRMed'95, Nice, France. April, pp. 3–12.

Grimson, W.E.L., Ettinger, G.J., White, S.J. et al., 1996. An automatic registration method for frameless stereotaxy, image guided surgery,

and enhanced reality visualization. IEEE Trans. Med. Imaging 15 (2), 129–140.

Hagemann, A., 2001. A Biomechanical Model of the Human Head with Variable Material Properties for Intraoperative Image Correction. PhD thesis, University of Hamburg. Logos, Berlin.

Hata, N., Nabavi, A., Warfield, S. et al., 1999. A volumetric optical flow method for measurement of brain deformation from intraoperative magnetic resonance images. In: Proceedings of MICCAI'99, September, pp. 928–935.

Hill, D., Maurer, C., Wang, M. et al., 1997. Estimation of intraoperative brain surface movement. In: Proceedings of CVRMed-MRCAS'97, Grenoble, France. March, pp. 449–458.

Hill, D.L.G., Maurer, C.R., Martin, A.J. et al., 1999. Assessment of intraoperative brain deformation using interventional MR imaging. In: Proceedings of MICCAI'99, September, pp. 910–919.

Kansy, K., Wisskirchen, P., Behrens, U. et al., 1999. LOCALITE: A frameless neuronavigation system for interventional magnetic resonance imaging systems. In: Proceedings of MICCAI'99, September, pp. 832–841.

Kyriacou, S.K., Davatzikos, C., 1998. A biomechanical model of soft tissue deformation, with application to non-rigid registration of brain images with tumor pathology. In: Proceedings of MICCAI'98, October, pp. 531–538.

Liseikin, V.D., 1999. Grid Generation Methods. Springer, Berlin.

Maurer, C.R., Hill, D.L.G., Maciunas, R.J. et al., 1998a. Measurement of intraoperative brain surface deformation under a craniotomy. In: Proceedings of MICCAI'98, October, pp. 51–62.

Maurer, C.R., Hill, D.L.G., Martin, A.J. et al., 1998b. Measurement of intraoperative brain deformation using a 1.5 Tesla interventional MR system: preliminary results. IEEE Trans. Med. Imaging 17 (5), 817–825.

Miga, M., Paulsen, K., Kennedy, F. et al., 1998. Initial in vivo analysis of 3D heterogeneous brain computations for model-updated image-guided neurosurgery. In: Proceedings of MICCAI'98, October, pp. 743–752.

Miga, M., Paulsen, K., Kennedy, F. et al., 1999. Model-updated image-guided neurosurgery using the finite element method: incorporation of the falx cerebri. In: Proceedings of MICCAI'99, September, pp. 900–909.

Miga, I.M., Staubert, A., Paulsen, D.K. et al., 2000. Model-updated image guided neurosurgery: preliminary analysis using intraoperative MR. In: Proceedings of MICCAI'2000, October, pp. 115–124.

Miller, K., Chinzei, K., 1997. Constitutive modelling of brain tissue: experiment and theory. J. Biomech. 30 (11/12), 1115–1121.

Nabavi, A., Black, P.McL., Gering, D.T. et al., 2001. Serial intraoperative MR imaging of brain shift. Neurosurgery 48 (4), 787–798.

Operation of the Mayfield® Acciss™ Stereotactic Workstation, QUICK REFERENCE, OMI® Surgical Products, March 1997.

Pamidi, M.R., Advani, S.H., 1978. Nonlinear constitutive relations for human brain tissue. J. Bio-Mech. Eng. 100, 44–48.

Peters, T., Davey, B., Munger, P. et al., 1996. Three-dimensional multimodal image-guidance for neurosurgery. IEEE Trans. Med. Imaging 15 (2), 121–128.

Press, W.H., Teukolsky, S.A., Vettrling, W.T., Flannery, B.P., 1992. Numerical Recipes in C, 2nd Edition. Cambridge University Press, Cambridge.

Reinges, M.H.T., Krombach, G., Nguyen, H. et al., 1997. Assessment of intraoperative brain tissue movements by frameless neuronavigation. Comput.-Aided Surg. 2, 218 (abstract).

Roberts, D.W., Hartov, A., Kennedy, F.E. et al., 1998. Intraoperative brain shift and deformation: a quantitative analysis of cortical displacement in 28 cases. Neurosurgery 43 (4), 749–760.

Škrinjar, O., Duncan, J., 1999. Real time 3D brain shift compensation. In: Proceedings of IPMI'99, June/July, pp. 42–55.

Škrinjar, O., Spencer, D., Duncan, J., 1998. Brain shift modeling for use in neurosurgery. In: Proceedings of MICCAI'98, October, pp. 641–649.

Škrinjar, O., Tagare, H., Duncan, S., 2000. Surface growing from stereo images. In: Proceedings of CVPR 2000, June, Vol. II, pp. 571–576.

Škrinjar, O., Studholme, C., Nabavi, A., Duncan, J., et al., 2001. Steps toward a stereo-camera-guided biomechanical model for brain shift compensation. In: Proceedings of IPMI'2001, June, pp. 183–189.

Stokking, R., 1998. Integrated Visualization of Functional and Anatomical Brain Images. PhD thesis, University Utrecht.

Studholme, C., Hill, D.L.G., Hawkes, D.J., 1996. Automated 3-D registration of MR and CT images of the head. Medical Image Analysis 1 (2), 163–175.

Studholme, C., Hawkes, D.J., Hill, D.L.G., 1998. A normalised entropy measure of 3D medical image alignment. SPIE Medical Imaging (February).

Valliappan, A., 1981. Continuum Mechanics Fundamentals. A.A. Balkema, Rotterdam.

Zienkiewicz, O.C., 1977. The Finite Element Method. McGraw-Hill, London.